Research Square

Preprints are preliminary reports that have not undergone peer review.
They should not be considered conclusive, used to inform clinical practice,
or referenced by the media as validated information.

Systems Immunology Network Analysis Identifies Candidate Regulators Associated with Divergent Responses to Infectious Bronchitis Virus in MBL-Selected Chicken Lines

Udayaraja GK
Aarhus University
Rikke Brødsgaard Kjaerup
Aarhus University
Edin Hamzic
Aarhus University
Nuria Mach-Casellas
INSTITUT NATIONAL DE LA RECHERCHE AGRONOMIQUE
Giuletta Minozzi
University of Milan
Albert Johannes Buitenhuis
Aarhus University
Xaquin Castro Dopico
Aarhus University
Tina Sørensen Dalgaard
Aarhus University
Haja N Kardarmideen
haja.k@anivet.au.dk

Aarhus University

Research Article

Keywords: Infectious bronchitis virus, Mannose-binding lectin, Gene co-expression network, Differential co-expression, Transcription factors, Chicken spleen transcriptome

Posted Date: November 19th, 2026

DOI: https://doi.org/10.21203/rs.3.rs-11595775/v1

License: This work is licensed under a Creative Commons Attribution 4.0 International License.
Read Full License

Additional Declarations: No competing interests reported.

Systems Immunology Network Analysis Identifies Candidate Regulators Associated with Divergent Responses to Infectious Bronchitis Virus in MBL-Selected Chicken Lines

Udayaraja GK[1], Rikke Brødsgaard Kjærup[1], Edin Hamzic[1], Nuria Mach-Casellas[4], Giuletta Minozzi[5], Albert Johannes Buitenhuis[3], Xaquin Castro Dopico[1], Tina Sørensen Dalgaard[1], Haja N Kardarmideen[1,2]*

[1]Department of Animal and Veterinary Sciences, Aarhus University, Tjele, Denmark

[2]Department of Molecular Biology and Genetics, Aarhus University, 8000 Aarhus, Denmark

[3]Center for Quantitative Genetics and Genomics, Aarhus University, 8000 Aarhus, Denmark

[4]INRA, UMR1313 GABI Animal Genetics and Integrative Biology, 78530 Jouy-en-Josas, Francek

[5]University of Milan, Department of Veterinary Medicine and Animal Sciences, Milan, Italy

Corresponding author: Haja N Kardarmideen, Aarhus University, Blichers Allé 20, 8830 Tjele, Denmark; haja.k@anivet.au.dk; 0000-0001-6294-382X

Abstract

Infectious bronchitis virus (IBV) causes major economic losses in poultry and host genetic variation in innate immunity influences the outcome of infection. Mannose-binding lectin (MBL), a soluble pattern-recognition molecule, is one such heritable factor. To investigate how the MBL-selected genetic background shapes the early splenic response to IBV, we applied an integrative systems immunology framework to spleen transcriptomes from two chicken lines divergently selected for high (L10H) and low (L10L) serum MBL, sampled one week after IBV challenge. Differential expression, parsimonious gene co-expression network analysis with intramodular hub identification, differential co-expression, transcription-factor annotation (AnimalTFDB) and association with measured immune phenotypes (serum MBL concentration, IBV-specific antibody titre and MHC haplotype) were combined to prioritise candidate genes supported by multiple independent lines of evidence. The low-MBL line showed a broader transcriptional response (436 versus 162 differentially expressed genes) and modestly more differential co-expression than the high-MBL line and yielded more multi-criteria candidates (13 versus 4). L10L candidates were enriched for transcription factors governing B-cell and plasma-cell differentiation, notably PRDM1 (BLIMP1), IRF4 and SOX4, together with immunoglobulin-related programmes, whereas the high-MBL line was characterised by complement-associated and cell-cycle transcription centred on C1QA and E2F8. These results indicate that divergent selection for serum MBL is associated with qualitatively different early antiviral strategies and nominate prioritised, validation-ready candidate genes linking innate immune background to the transcriptional response to IBV.

Keywords Infectious bronchitis virus · Mannose-binding lectin · Gene co-expression network · Differential co-expression · Transcription factors · Chicken spleen transcriptome

Introduction

Infectious bronchitis virus (IBV) is a highly contagious avian coronavirus and remains one of the most economically important viral pathogens in the poultry industry, causing respiratory disease, nephritis, reduced egg production and impaired growth performance (Cook et al., 2012, Jackwood, 2012). Host resistance to IBV requires a complex interplay between innate and adaptive immune responses, but the regulatory mechanisms that coordinate these responses are not yet fully understood. Mannose binding lectin (MBL) is a soluble pattern-recognition molecule of the innate immune system that among others recognises carbohydrate structures on invading pathogens and e.g. activates the lectin complement pathway, playing a role in early antiviral defence (Eisen and Minch, 2018, Thiel et al., 1997) but may also play a role in development of adaptive immune responses (Downing et al., 2003). Interestingly, MBL deficiency in humans, commonly caused by mutations in the human *MBL2* gene, is associated with increased susceptibility to respiratory viral infections in young children. In contrast, MBL deficiency may also be protective against parasitic infections, potentially contributing to the persistence of MBL-deficiency alleles in certain African human populations (Turner, 2003).

As in mammals, baseline MBL levels in peripheral blood are genetically determined (Kjaerup et al., 2014a, Kjaerup et al., 2013). To elucidate the role of innate immune background in antiviral immunity, the AU L10H and L10L inbred chicken lines (derived from the UM-B19/White Cornish population) were divergently selected over several generations for high (L10H) and low (L10L) serum MBL concentrations, providing a unique genetic model to study the influence of MBL-associated innate immunity on experimental infection responses (Juul-Madsen et al., 2003, Juul-Madsen et al., 2007).

Previous studies of IBV infected L10 chickens report distinct acute phase responses with a two-fold increase in MBL plasma levels peaking around day 3 post infection but differential responses with L10H in general displaying lower viral loads in the upper respiratory tract, and a single study even showed that L10H viral load peaked earlier and was cleared faster than in L10L chickens (Juul-Madsen et al., 2007, Kjaerup et al., 2014a).

We have previously investigated whether the genetic variation in MBL-associated innate immune competence influences the transition from early antiviral responses to adaptive immune activation following IBV infection in generation 14 of the L10 chickens (Kjaerup et al.,

2014b, Hamzić et al., 2016). Apart from lower viral load in infected L10H chickens, also extrahepatic production of MBL was evident in the lungs of L10H chickens (Kjaerup et al., 2014b) combined with less IBV induced tracheal damage. The spleen transcriptome of animals from this study interestingly also revealed differences in expression of genes belonging to adaptive immune responses (Hamzić et al., 2016). We therefore hypothesised that the two lines engage different candidate genes during infection, and the present study aimed to characterise these divergent immune trajectories.

Differential expression analysis can reveal genes with altered transcript abundance, but it treats genes individually and thus cannot capture the coordinated transcriptomic network and identify the regulatory mechanisms underlying complex immune responses. In gene co-expression network studies, functional modules and hub genes capture coordinated biological processes across samples (Langfelder and Horvath, 2008, Paci et al., 2021). Differential co-expression studies may indicate transcriptional network rewiring even with small gene expression changes. Together, these network-based approaches provide insight into dynamic regulatory organisation that cannot be inferred from conventional differential expression analysis alone.

Transcription factors (TFs) are major regulators of antiviral immunity, coordinating interferon signalling, cytokine production, lymphocyte differentiation, and immune cell activation. Integrating TF annotation with co-expression modules can therefore help to identify candidate upstream regulators of lineage-specific immune responses. In addition, connecting transcriptomic networks with measured immune phenotypes enables identification of pathways associated with both innate and adaptive immunity. Genes involved in antiviral defence and immune regulation include regulators of type I interferon responses (e.g., IRF7, STAT2, IFI6, IFI27L2), B-cell differentiation and antibody production (PRDM1, IRF4, BCL6), T-cell development and activation (SOX4, STAT3) and complement activation (C1QA) and thus represent attractive candidates for systems-level investigation (Chaplin, 2010, St. Leger et al., 2022).

Here, we present an integrative systems immunology framework that combines differential expression, parsimonious co-expression network analysis, intramodular hub gene identification, differential co-expression, TF regulatory analysis, and functional enrichment with measured immune phenotypes, including serum MBL concentration, IBV-specific antibody titre, and MHC haplotype. Integrated systems-level transcriptome analysis is a powerful approach to study host–pathogen interactions and identify key biological regulators (Barabási et al., 2011, Ideker and Krogan, 2012). Using spleen transcriptomes collected one week after IBV challenge, we investigate how genetically divergent MBL-selected chicken lines reorganise their transcriptional networks during early infection and identify candidate genes linking innate

immune background to the response to infection. By integrating complementary evidence (candidates require ≥3 of five evidence criteria) rather than analysing genes in isolation, this framework recovers established immune regulators while also highlighting less well-characterised genes and infection-associated changes in co-expression linked to the divergent responses. We hypothesised that the high- and low-MBL lines, which differ in their response to IBV infection, show distinct splenic gene co-expression network architectures, with immune-related modules and hub genes that differ between the lines. To address this hypothesis, the study had two specific objectives: (i) to construct gene co-expression networks and identify the key modules and intramodular hub genes associated with the differential immune responses between the high- and low-MBL chicken lines and (ii) to characterise the immunological pathways associated with the MBL-related difference in host response, and to prioritise candidate genes associated with the divergent responses to IBV.

Materials and methods

2.1 Transcriptomic dataset and immune phenotype integration

The RNA-sequencing data were obtained from the study of (Hamzić et al., 2016). This dataset comprises 63 spleen transcriptomes from the AU L10H and L10L inbred chicken lines divergently selected for high (L10H) and low (L10L) serum mannose-binding lectin (MBL) concentrations. These libraries were generated from birds experimentally challenged with infectious bronchitis virus (IBV) and sampled at one and three weeks post-infection, together with matched uninfected controls, forming a 2 × 2 × 2 factorial experimental design. Raw reads were quality-checked (Withanage et al., 2022) and adapter-trimmed with Trim Galore v0.6.10 (Krueger et al., 2023) and aligned with STAR v2.7.11a (Dobin et al., 2013) to the Gallus gallus reference assembly GRCg7b (Ensembl release 115). Alignments were processed with SAMtools v1.23 and gene-level read counts were obtained with featureCounts v2.1.1 (Danecek et al., 2021, Liao et al., 2014). Transcriptomic profiles were integrated with individual immune phenotypes reported in the original study, including serum MBL concentration (μg ml^{-1}; pre-challenge baseline, day −1/0), IBV-specific antibody titre measured seven days post-infection, and major histocompatibility complex (MHC; B-locus) haplotype. Sample identities were linked deterministically between the published phenotype table and RNA-seq data using the original RNA-seq sample identifiers, with all mappings verified against experimental metadata (genetic line, infection status and sampling week).

2.2 Differential expression and transcriptional network analysis

Differential gene expression between infected and control birds was analysed independently within each chicken line using DESeq2 v1.50.2 (R v4.5.2) (Love et al., 2014), which estimates gene-wise dispersion using a negative binomial generalised linear model following size-factor normalisation and empirical Bayes shrinkage of dispersion estimates. Statistical significance was assessed using Wald tests with Benjamini–Hochberg false-discovery rate (FDR) correction (Benjamini and Hochberg, 1995), and genes with adjusted $P < 0.05$ were considered differentially expressed. To facilitate downstream functional analyses, genes were additionally ranked using the signed statistic, which preserves both effect direction and statistical significance. Unless otherwise stated, differentially expressed gene counts refer to this adjusted-P threshold alone; where genes were partitioned into up- and down-regulated sets (for example for functional enrichment and heatmaps), an additional effect-size threshold of $|\log2 \text{ fold-change}| \geq 1$ was applied.

To characterise coordinated transcriptional programmes beyond individual gene responses, condition-specific gene co-expression networks were constructed using Parsimonious Gene Correlation Network Analysis (PGCNA2)(Care et al., 2019). Briefly, pairwise Spearman correlations were calculated between expressed genes and the strongest correlations retained using the edge-per-gene strategy implemented in PGCNA2 (three edges retained per gene; retention fraction 1.0; [Leiden resolution/iterations]), producing sparse yet biologically informative correlation networks. Community detection was performed using the Leiden optimisation algorithm (Traag et al., 2019), yielding transcriptional modules representing groups of coordinately regulated genes. Module activity was summarised by eigengenes, calculated as the first principal component of scaled $\log_2$-transformed expression values and sign-aligned to the average module expression profile.

Because PGCNA2 constrains node connectivity through fixed edge retention, conventional degree centrality provides limited discrimination of biologically important genes. Instead, intramodular hub genes were identified using module membership (kME), defined as the Pearson correlation between each gene and its corresponding module eigengene. The 25 genes with the highest absolute kME in each module, calculated within the samples of the corresponding condition, were designated intramodular hub genes (Langfelder and Horvath, 2008).

2.3 Network rewiring and immune phenotype association

To identify transcriptional reorganisation induced by IBV infection, differential co-expression was assessed within each line using a link-based differential co-expression framework (Tesson et al., 2010). So that the two lines could be compared directly, both were analysed on a

common gene universe comprising the 2,000 genes with the highest expression variance across all week-1 samples. Within each line, Spearman correlations were calculated separately for control and infected birds (L10L, n = 8 and 7; L10H, n = 8 and 8). A gene pair was treated as a qualified link if $|\rho| \geq 0.5$ in at least one condition, and as a differentially co-expressed link (DCL) if, in addition, $|\rho_{control} - \rho_{infected}| \geq 0.5$ and the Fisher z-test for the difference between the two correlations was significant after Benjamini–Hochberg correction ($q < 0.10$). A gene was classified as a differentially co-expressed gene (DCG) when its qualified links were enriched for DCLs relative to the overall DCL rate (one-sided binomial test, Benjamini–Hochberg $q < 0.10$, at least one DCL).

To associate transcriptional organisation with immune phenotypes, module gene sets defined in each condition-specific network were summarised as eigengenes across all birds of the corresponding line (control and infected; L10L n = 15, L10H n = 16), thereby maximising statistical power; because infected and control birds were pooled, these correlations may partly reflect infection status. Module eigengenes were correlated with continuous immune traits (serum MBL concentration and IBV antibody titre) (Kjaerup et al., 2014b) using Spearman's rank correlation, with FDR correction applied across tested modules. Associations with categorical MHC haplotypes were evaluated using one-way analysis of variance (ANOVA), and effect sizes were quantified using eta-squared (η^2). At the individual gene level, gene significance (GS) was defined as the Spearman correlation between gene expression and each immune phenotype, with genes exhibiting nominal $P < 0.05$ considered phenotype-associated for subsequent integrative analyses. These gene–trait associations are nominal and uncorrected for multiple testing, and were therefore treated as an exploratory evidence layer for candidate prioritisation rather than as statistically confirmed relationships. Eigengene, module-membership, correlation, differential co-expression and integration analyses were performed in Python v3.10.12 using NumPy v2.2.6, pandas v2.3.3, SciPy v1.15.3 and scikit-learn v1.7.2.

2.4 Integration of evidence criteria and functional characterisation

To prioritise candidate genes associated with the divergent responses, five complementary evidence criteria were combined: (i) differentially expressed genes (DEGs), (ii) intramodular hub genes, (iii) differentially co-expressed genes (DCGs), (iv) transcription factors, defined as expressed genes whose gene symbol matched one of the 1,058 Gallus gallus TFs in the Animal Transcription Factor Database (AnimalTFDB) v4.0 (Shen et al., 2023), yielding 689 TFs (symbol matching was required because AnimalTFDB uses gene identifiers from the previous chicken genome assembly), and (v) immune phenotype-associated genes. Genes meeting three or more of these five criteria were prioritised as candidate genes.

Biological interpretation of DEGs, co-expression modules and prioritised candidate genes was performed using functional enrichment analysis in DAVID (Database for Annotation,

Visualisation and Integrated Discovery; web service accessed in 2026) (Huang da et al., 2009), interrogating Gene Ontology Biological Process, Cellular Component and Molecular Function ontologies together with KEGG (Chen et al., 2017) and Reactome pathway databases. Statistical significance was determined using Benjamini-adjusted P values < 0.05. Gene annotation was based on Ensembl release 115 (GRCg7b). Gene identifiers lacking approved gene symbols were retained throughout all analyses to avoid excluding poorly annotated but potentially functional loci.

Results

3.1 Distinct transcriptional responses to IBV infection in genetically divergent MBL-selected lines

To investigate how genetic background influences the early splenic response to IBV infection, we integrated differential expression, co-expression network analysis, differential co-expression, TF analysis, and immune phenotype association into a unified systems-level framework (Fig. 1). Despite both chicken lines being challenged under identical experimental conditions, their transcriptomic responses differed substantially (Supplementary Fig. S1). The low-MBL (L10L) line exhibited approximately threefold more DEGs than the high-MBL (L10H) line (436 vs 162), a moderately larger number of differentially co-expressed genes (42 vs 28) and a larger set of candidate genes supported by multiple evidence criteria (13 vs 4; Table 1). In both lines the infection response was more pronounced at week 1 than at week 3 (Fig. 2A). Downstream analyses were focused on the week-1 time point, as day 7 (week 1) is the earliest available spleen RNA-seq time point, capturing an early phase in which innate responses are transitioning towards adaptive immunity, to characterise the early system-level transcriptional response to infection. Heatmaps of the top significant DEGs (padj < 0.05) comparing infected and control samples for L10L and L10H are shown in Fig 2B and Fig 2C, respectively.

3.2 MBL-associated transcriptional modules reveal distinct biological programmes

Gene co-expression analysis identified multiple transcriptional modules in each experimental condition, several of which were associated with measured immune phenotypes. As previously reported, serum MBL concentrations showed a classical acute phase response in both chicken lines with first a two-fold increase peaking at around day 3 pi followed by a marked decrease, reaching a nadir (below baseline) around day 7 pi and returning to base-line levels at around day 21 pi (Kjaerup et al., 2014b). Across both genetic lines, serum MBL concentration showed the strongest relationship with module activity. In the infected networks, the leading module in each line was negatively correlated with serum MBL concentration, indicating transcriptional programmes that were more active in birds with lower baseline serum MBL. Although these

associations did not remain significant following multiple-testing correction because of the limited sample size (n = 15–16 per line), they were interpreted together with the convergent evidence from hub-gene analysis and functional enrichment.

Functional annotation demonstrated that the MBL-associated modules represented fundamentally different biological processes in the two genetic backgrounds. In the L10L infected network, the MBL-anticorrelated module (M4) was strongly enriched for ribosome biogenesis and translation-related processes (Benjamini-adjusted $P = 5 \times 10^{-27}$), consistent with extensive activation of protein synthesis during the early antiviral response. The MBL-associated module in L10H (M2) was strongly enriched for genes involved in cell-cycle progression and proliferation (Benjamini-adjusted $P = 3 \times 10^{-15}$), noting that proliferation may itself reflect immune-cell activation and expansion. L10H up-regulated genes are involved in lysosomal antigen processing and proteolysis, while L10L up-regulated genes are involved in immunoglobulin synthesis and endoplasmic reticulum protein-processing (Table 2). Pathway enrichment analysis of up-regulated genes confirmed this divergence, the L10L response was dominated by immunoglobulin complex, antigen-binding and endoplasmic-reticulum protein-processing pathways, whereas the L10H response was enriched for lysosomal and cysteine-type endopeptidase (cathepsin) pathways (Fig. 3).

3.3 Hub genes and differential network rewiring identify distinct regulatory programmes

Intramodular hub genes, defined by their strong correlation with module eigengenes, identified candidate regulators underlying the MBL-associated transcriptional programmes. In the high-MBL line, the leading infected module was centred on E2F8, which exhibited the highest module membership (kME = 0.97) and a strong negative correlation with serum MBL concentration ($\rho = -0.82$). Additional highly connected genes PARP1, a key regulator of DNA damage response and repair, together with DDX24, an RNA helicase involved in RNA processing, and METAP1, which contributes to protein maturation, formed prominent hubs, consistent with enrichment of cell-cycle and DNA replication pathways (Fig. 4). In contrast, the corresponding low-MBL module was organised around AP3B2 (a subunit of the AP-3 adaptor complex involved in vesicle trafficking), OSER1 (an oxidative-stress-responsive gene) and HNRNPD/AUF1 (an AU-rich-element mRNA-stability factor that can modulate the turnover of inflammatory transcripts). These are not canonical immune regulators; their emergence as intramodular hubs is therefore interpreted as a data-driven observation requiring experimental confirmation rather than as evidence of an established immune function.

Differential co-expression analysis on the common gene universe identified 42 DCGs (4,755 differentially co-expressed links) in L10L and 28 DCGs (3,431 links) in L10H (Table 1), indicating

infection-associated reorganisation of gene–gene correlation in both lines that was modestly greater in the low-MBL background. None of the DCGs met the criteria for the final candidate sets (Section 3.4).

3.4 Integration of evidence criteria prioritises candidate genes associated with the divergent responses

Integration of differential expression, co-expression network topology, differential co-expression, transcription factor annotation and immune phenotype association identified distinct regulatory architectures in the two chicken lines (Fig. 5). Requiring support from at least three of the five evidence criteria prioritised 13 candidate genes in the L10L line, compared with only four genes in L10H (Table 1), consistent with the broader response observed in the low-MBL line.

Twelve of the 13 L10L candidates were TFs, including PRDM1 (BLIMP1), IRF4 and SOX4, each of which was differentially expressed, annotated as a TF and associated with at least one immune phenotype. Because TF annotation was itself one of the five criteria, this predominance of TFs partly reflects the prioritisation rule rather than being an independent finding. None of the 17 candidates across both lines was a DCG, so the final candidate sets reflect support from the other four criteria (Table S1). These regulators were accompanied by an immunoglobulin-rich transcriptional programme consistent with activation of adaptive immune responses. In contrast, the smaller L10H candidate set comprised the complement component C1QA (a hub that was differentially expressed and immune-associated), the transcription factors E2F8 and ZNF367 (hubs that were not differentially expressed) and TMEM268, consistent with a more contained, innate-leaning response featuring complement-associated and proliferative transcription. Collectively, these findings indicate that divergent selection for serum MBL concentration is associated with different early response profiles, which may reflect differences in response strategy or in infection kinetics. At day 7 pi the low-MBL line showed a broad response whose candidates include adaptive-immune transcription factors, whereas the high-MBL line showed a more restricted, innate-leaning profile.

Discussion

The host response to viral infection emerges from coordinated interactions among thousands of genes rather than changes in the expression of individual transcripts. By integrating differential expression, co-expression networks, differential co-expression, TF analysis and measured immune phenotypes, our system-level framework revealed regulatory programmes underlying the early splenic response to IBV that were not apparent from conventional gene-by-gene analysis alone. Although the original transcriptomic study identified infection-

associated differential expression between the MBL-selected chicken lines (Hamzić et al., 2016) our network-based analysis shows that the two genetic backgrounds also differ in how infection-responsive genes are organised into co-expression modules, hubs and phenotype-associated programmes. Network-level analyses can reveal coordinated changes that are not apparent from gene-by-gene comparisons (de la Fuente, 2010, Ideker and Krogan, 2012).

The low-MBL (L10L) line exhibited greater transcriptional plasticity than the high-MBL (L10H) line in the spleen at day 7 pi, characterised by a larger number of differentially expressed genes, more differential co-expression and a broader set of candidate genes supported by multiple evidence criteria. Particularly notable was the prioritisation of the TFs PRDM1 (BLIMP1), IRF4, and SOX4, together with enrichment of immunoglobulin-related pathways. PRDM1 and IRF4 regulate B-cell differentiation and plasma-cell maturation, promoting antibody-secreting cells and humoral immunity (Nutt et al., 2015, Yu and Lin, 2016). SOX4 is also involved in lymphocyte development and differentiation of adaptive immune cells (Sun et al., 2013). One interpretation of the convergence of these transcription factors with immunoglobulin-associated genes is that birds with low constitutive MBL engage adaptive immune programmes earlier to compensate for weaker innate pathogen recognition; alternatively, the broader response may reflect a higher antigen burden in this line (see limitations). Higher viral loads in the L10L line (Hamzić et al., 2016, Kjaerup et al., 2014b) would provide a stronger stimulus for B-cell-mediated responses.

The high-MBL line had a more muted transcriptional response with fewer differentially expressed genes, modest network reconfiguration and few prioritised candidates. Functional enrichment revealed preferential activation of innate immune systems via lysosomal antigen processing and C1QA. This is biologically plausible because MBL and C1q belong to the collectin/C1q superfamily of pattern-recognition molecules and initiate closely related complement activation pathways through the lectin and classical pathways, respectively (Garred et al., 2016, Ricklin et al., 2016). Higher constitutive MBL concentrations may therefore enable more efficient pathogen recognition immediately after infection, which could reduce the need for extensive downstream transcriptional remodelling while maintaining complement-mediated defence. The identification of C1QA as the principal multi-criteria candidate in L10H further supports the importance of complement-associated transcription as a defining feature of the early antiviral response in birds with enhanced innate immune capacity.

Despite these contrasting regulatory strategies, both genetic backgrounds shared a prominent transcriptional module whose activity was negatively associated with circulating MBL concentration. Although the biological identity of this module differed between lines, being enriched for translational processes in L10L and cell-cycle progression in L10H, both programmes are consistent with increased biosynthetic or proliferative activity during infection.

This common relationship suggests that birds with lower constitutive (baseline) MBL show greater splenic biosynthetic or proliferative activity during infection, regardless of the underlying molecular programme. Within the high-MBL network, the transcription factor E2F8 emerged as the dominant intramodular hub, linking cell-cycle regulation with MBL-associated module activity. Members of the E2F family regulate cell proliferation, DNA replication and differentiation in both immune and non-immune tissues (Kent and Leone, 2019) making E2F8 a compelling candidate connecting innate immune background with proliferative responses during IBV infection.

One major finding of this study is that a number of the top candidate genes were identified not only through differential expression but also through network topology and association with phenotypes. Several candidates, including E2F8 and ZNF367 in L10H and ZNF366 and ZNF767 in L10L, were not differentially expressed but were prioritised through their module centrality together with TF annotation and phenotype association. These cases illustrate that network position can add information not captured by transcript abundance alone (Ideker and Krogan, 2012, Langfelder and Horvath, 2008). In addition, the integration of multiple evidence criteria substantially reduced the search space for candidate genes, generating a focused set of biologically plausible candidates for experimental validation.

The present study has several limitations. First, the analysis was restricted to the one-week post-infection time point, representing an early phase of the antiviral response where transition of innate to adaptive programmes may occur. Longitudinal integration of transcriptomes from multiple time points together with leukocyte subset measurements may provide additional insight into the transition from innate to adaptive immunity. Second, the relatively modest sample size limits statistical power for phenotype association analyses, and therefore module-trait relationships should be interpreted alongside the convergent evidence obtained from network topology, differential co-expression and functional enrichment. Third, the inferred regulatory interactions are correlative and require experimental validation using targeted functional approaches. Fourth, spleen RNA-seq measures bulk tissue, so some between-line differences in transcript abundance may reflect differences in cellular composition (for example relative lymphocyte, monocyte or plasma-cell proportions) rather than cell-intrinsic regulation; cell-sorted or deconvolution approaches would be required to resolve this. Relatedly, because L10H birds carry lower tracheal viral loads at this time point, part of the between-line transcriptional divergence may reflect differences in antigen burden and infection kinetics rather than the MBL-selected background per se. Fifth, the per-line co-expression and differential co-expression networks were inferred from small samples (n = 15–16) and network-stability procedures such as leave-one-out or bootstrap resampling were not performed, so the hub and rewiring results should be regarded as exploratory. In addition, IBV-specific antibody titres at day 7 pi were low and right-skewed, and MHC haplotypes were strongly unbalanced

across birds, which limits the power of these phenotype associations. Finally, the differential co-expression criterion did not contribute to any final candidate, so the prioritised genes rest on the remaining four criteria.

In summary, our integrative systems immunology framework indicates that divergent selection for serum MBL concentration is associated with different early transcriptional responses to IBV. The low-MBL line showed a broader response whose prioritised candidates include B-cell and plasma-cell transcription factors, whereas the high-MBL line showed a more restricted response featuring complement-associated and cell-cycle genes. By integrating transcript abundance, network architecture and immune phenotypes, this study extends previous transcriptomic analyses and provides a candidate-prioritisation framework for identifying candidate genes linking genetic background to the antiviral response. The prioritised candidates, including PRDM1, IRF4, SOX4, C1QA, and E2F8, represent targets for functional validation and, if confirmed, could inform genetic selection for disease resistance in poultry.

Conclusion

Systems-level integration shows that the MBL-divergent chicken lines differ in their early splenic transcriptional response to IBV infection: a broader response featuring transcription factors in the low-MBL line and a more restricted, complement- and cell-cycle-associated response in the high-MBL line. The analysis converges on a small set of candidate genes (PRDM1, IRF4 and SOX4; C1QA and E2F8). These candidates and the line-dependent network architecture provide concrete, testable hypotheses for how selection on a single innate trait may shape antiviral immunity.

Declarations:

Funding: This work was supported by internal Department of Animal and Veterinary Sciences funding from Aarhus University, Denmark

Competing interests: The authors declare no competing interests

Ethics approval: The experimental procedures were conducted under the protocols approved by the Danish Animal Experiments Inspectorate and complied with the Danish Ministry of Justice Law no. 382 (June 10, 1987) and Acts 739 (December 6, 1988) and 333 (May 19, 1990) concerning animal experimentation and care of experimental animals. The license to conduct the animal experiment was obtained by Helle R. Juul-Madsen.

Consent to participate: Not applicable.

Consent for publication: Not applicable.

Clinical trial number: Not applicable

Availability of data and materials: The RNA-sequencing dataset analysed in this study is available from the NCBI Gene Expression Omnibus (GEO) under accession GSE73423 (BioProject PRJNA296924; SRA runs SRR2516421–SRR2516484). Supplementary Fig. S1 and derived tables are provided as Supplementary Material.

Code availability: Analytics scripts and derived tables are available from the corresponding author on reasonable request.

Author contributions:

UGK: Software, formal analysis, visualization, writing - original draft. RBK, EH, NM, GM, AB, and XCD: Writing - review and editing. TSD: Project administration, methodology, data curation, funding acquisition, writing - review and editing. HNK: Conceptualization, methodology, project administration, supervision, writing - review and editing.

Acknowledgements:

The authors gratefully acknowledge Eva Wattrang, Liselotte R. Norup, Valentina Gualdi, John L. Williams, Jun Chen, and Francesco Strozzi for their contributions to the previous work that supported the development of this study.

References

BARABÁSI, A.-L., GULBAHCE, N. & LOSCALZO, J. 2011. Network medicine: a network-based approach to human disease. *Nature Reviews Genetics,* 12**,** 56–68.

BENJAMINI, Y. & HOCHBERG, Y. 1995. Controlling the False Discovery Rate - a Practical and Powerful Approach to Multiple Testing. *Journal of the Royal Statistical Society Series B-Statistical Methodology,* 57**,** 289–300.

CARE, M. A., WESTHEAD, D. R. & TOOZE, R. M. 2019. Parsimonious Gene Correlation Network Analysis (PGCNA): a tool to define modular gene co-expression for refined molecular stratification in cancer. *Npj Systems Biology and Applications,* 5.

CHAPLIN, D. D. 2010. Overview of the immune response. *Journal of Allergy and Clinical Immunology,* 125**,** S3–S23.

CHEN, L., ZHANG, Y. H., WANG, S., ZHANG, Y., HUANG, T. & CAI, Y. D. 2017. Prediction and analysis of essential genes using the enrichments of gene ontology and KEGG pathways. *PLoS One,* 12**,** e0184129.

COOK, J. K. A., JACKWOOD, M. W. & JONES, R. C. 2012. The long view: 40 years of infectious bronchitis research. *Avian Pathology,* 41**,** 239–250.

DANECEK, P., BONFIELD, J. K., LIDDLE, J., MARSHALL, J., OHAN, V., POLLARD, M. O., WHITWHAM, A., KEANE, T., MCCARTHY, S. A., DAVIES, R. M. & LI, H. 2021. Twelve years of SAMtools and BCFtools. *Gigascience,* 10.

DE LA FUENTE, A. 2010. From 'differential expression' to 'differential networking' — identification of dysfunctional regulatory networks in diseases. *Trends in Genetics,* 26**,** 326–333.

DOBIN, A., DAVIS, C. A., SCHLESINGER, F., DRENKOW, J., ZALESKI, C., JHA, S., BATUT, P., CHAISSON, M. & GINGERAS, T. R. 2013. STAR: ultrafast universal RNA-seq aligner. *Bioinformatics,* 29**,** 15–21.

DOWNING, I., KOCH, C. & KILPATRICK, D. C. 2003. Immature dendritic cells possess a sugar-sensitive receptor for human mannan-binding lectin. *Immunology,* 109**,** 360–364.

EISEN, D. P. & MINCH, K. 2018. Impact of mannose-binding lectin on susceptibility to infectious diseases. *Clinical Infectious Diseases,* 66**,** 772–779.

GARRED, P., GENSTER, N., PILELY, K., BAYARRI-OLMOS, R., ROSBJERG, A., MA, Y. J. & SKJOEDT, M. O. 2016. A journey through the lectin pathway of complement-MBL and beyond. *Immunol Rev,* 274**,** 74–97.

HAMZIĆ, E., KJÆRUP, R. M. & JUUL-MADSEN, H. R. 2016. Integrated spleen transcriptome responses to infectious bronchitis virus in two chicken lines divergently selected for serum mannose-binding lectin levels. *BMC Genomics,* 17**,** 82.

HUANG DA, W., SHERMAN, B. T. & LEMPICKI, R. A. 2009. Systematic and integrative analysis of large gene lists using DAVID bioinformatics resources. *Nat Protoc,* 4**,** 44–57.

IDEKER, T. & KROGAN, N. J. 2012. Differential network biology. *Molecular Systems Biology,* 8**,** 565.

JACKWOOD, M. W. 2012. Review of infectious bronchitis virus around the world. *Avian Diseases,* 56**,** 634–641.

JUUL-MADSEN, H. R., MUNCH, M., HANDBERG, K. J., SORENSEN, P., JOHNSON, A. A., NORUP, L. R. & JORGENSEN, P. H. 2003. Serum levels of mannan-binding lectin in chickens prior to and during experimental infection with avian infectious bronchitis virus. *Poult Sci,* 82**,** 235–41.

JUUL-MADSEN, H. R., NORUP, L. R., HANDBERG, K. J. & JORGENSEN, P. H. 2007. Mannan-binding lectin (MBL) serum concentration in relation to propagation of infectious bronchitis virus (IBV) in chickens. *Viral Immunol,* 20**,** 562–70.

KENT, L. N. & LEONE, G. 2019. The broken cycle: E2F dysfunction in cancer. *Nat Rev Cancer,* 19**,** 326–338.

KJAERUP, R. M., DALGAARD, T. S., NORUP, L. R., GOTO, R. M., MILLER, M. M., SORENSEN, P. & JUUL-MADSEN, H. R. 2014a. Transcription efficiency of different chicken mannose-binding lectin promoter alleles. *Immunogenetics,* 66**,** 737–42.

KJAERUP, R. M., DALGAARD, T. S., NORUP, L. R., HAMZIC, E., SORENSEN, P. & JUUL-MADSEN, H. R. 2014b. Characterization of cellular and humoral immune responses after IBV infection in chicken lines differing in MBL serum concentration. *Viral Immunol,* 27**,** 529–42.

KJAERUP, R. M., NORUP, L. R., SKJODT, K., DALGAARD, T. S. & JUUL-MADSEN, H. R. 2013. Chicken mannose-binding lectin (MBL) gene variants with influence on MBL serum concentrations. *Immunogenetics,* 65**,** 461–71.
KRUEGER, F., JAMES, F., EWELS, P., AFYOUNIAN, E., WEINSTEIN, M., SCHUSTER-BOECKLER, B. & HULSELMANS, G. 2023. FelixKrueger/TrimGalore: v0. 6.10-add default decompression path. *Zenodo*.
LANGFELDER, P. & HORVATH, S. 2008. WGCNA: an R package for weighted correlation network analysis. *BMC Bioinformatics,* 9**,** 559.
LIAO, Y., SMYTH, G. K. & SHI, W. 2014. featureCounts: an efficient general purpose program for assigning sequence reads to genomic features. *Bioinformatics,* 30**,** 923–30.
LOVE, M. I., HUBER, W. & ANDERS, S. 2014. Moderated estimation of fold change and dispersion for RNA-seq data with DESeq2. *Genome Biol,* 15**,** 550.
NUTT, S. L., HODGKIN, P. D., TARLINTON, D. M. & CORCORAN, L. M. 2015. The generation of antibody-secreting plasma cells. *Nat Rev Immunol,* 15**,** 160–71.
PACI, P., FISCON, G., CONTE, F., WANG, R.-S., FARINA, L. & LOSCALZO, J. 2021. Gene co-expression in the interactome: moving from correlation toward causation via an integrated approach. *Network and Systems Medicine,* 4**,** 76–90.
RICKLIN, D., REIS, E. S. & LAMBRIS, J. D. 2016. Complement in disease: a defence system turning offensive. *Nat Rev Nephrol,* 12**,** 383–401.
SHEN, W. K., CHEN, S. Y., GAN, Z. Q., ZHANG, Y. Z., YUE, T., CHEN, M. M., XUE, Y., HU, H. & GUO, A. Y. 2023. AnimalTFDB 4.0: a comprehensive animal transcription factor database updated with variation and expression annotations. *Nucleic Acids Res,* 51**,** D39–D45.
ST. LEGER, A. J., PREVITE, D. M. & DANA, M. R. 2022. T Lymphocyte Responses. *Albert and Jakobiec's Principles and Practice of Ophthalmology*. Springer.
SUN, B., MALLAMPATI, S., GONG, Y., WANG, D., LEFEBVRE, V. & SUN, X. 2013. Sox4 is required for the survival of pro-B cells. *J Immunol,* 190**,** 2080–9.
TESSON, B. M., BREITLING, R. & JANSEN, R. C. 2010. DiffCoEx: a simple and sensitive method to find differentially coexpressed gene modules. *BMC Bioinformatics,* 11**,** 497.
THIEL, S., HOLMSKOV, U. & HVIID, L. 1997. The concentration of the C-type lectin, mannan-binding protein, in human plasma increases during an acute phase response. *Clinical and Experimental Immunology,* 90**,** 31–35.
TRAAG, V. A., WALTMAN, L. & VAN ECK, N. J. 2019. From Louvain to Leiden: guaranteeing well-connected communities. *Sci Rep,* 9**,** 5233.
TURNER, M. W. 2003. The role of mannose-binding lectin in health and disease. *Mol Immunol,* 40**,** 423–9.
WITHANAGE, M. H. H., LIANG, H. & ZENG, E. 2022. RNA-Seq Experiment and Data Analysis. *Methods Mol Biol,* 2418**,** 405–424.
YU, Y. H. & LIN, K. I. 2016. Factors That Regulate the Generation of Antibody-Secreting Plasma Cells. *Adv Immunol,* 131**,** 61–99.

Tables

Table 1. Number of genes meeting each evidence criterion (week 1, per line).

Layer	L10L (low-MBL)	L10H (high-MBL)
DEGs (infected vs control, padj < 0.05)	436	162
Differentially co-expressed genes (q < 0.10; common top-2,000 genes)	42	28
Transcription factors (mapped)	689	689
Immune-trait-associated genes (GS p < 0.05)	1,906	1,508
Co-expression modules	control 11 / infected 5	control 7 / infected 7
Prioritised candidates (≥ 3 of 5 criteria)	13	4

Table 2. Functional identity (top functional enrichment) of key gene sets per line. The last row is descriptive; the candidate sets are too small for enrichment testing.

Gene set	L10L (low-MBL)	L10H (high-MBL)
Infected lead module (MBL-anticorrelated)	ribosome / translation	cell cycle / proliferation
Infection up-regulated genes	immunoglobulin / antigen binding; ER protein processing	lysosome / cathepsin antigen processing
Immune-trait-associated genes	lysosome / endosome / antigen processing	broad (49 terms)
Prioritised candidates (descriptive)	B-cell/plasma-cell and developmental TFs (PRDM1, IRF4, SOX4, BCL6)	complement (C1QA) and cell-cycle TFs (E2F8, ZNF367)

Figures

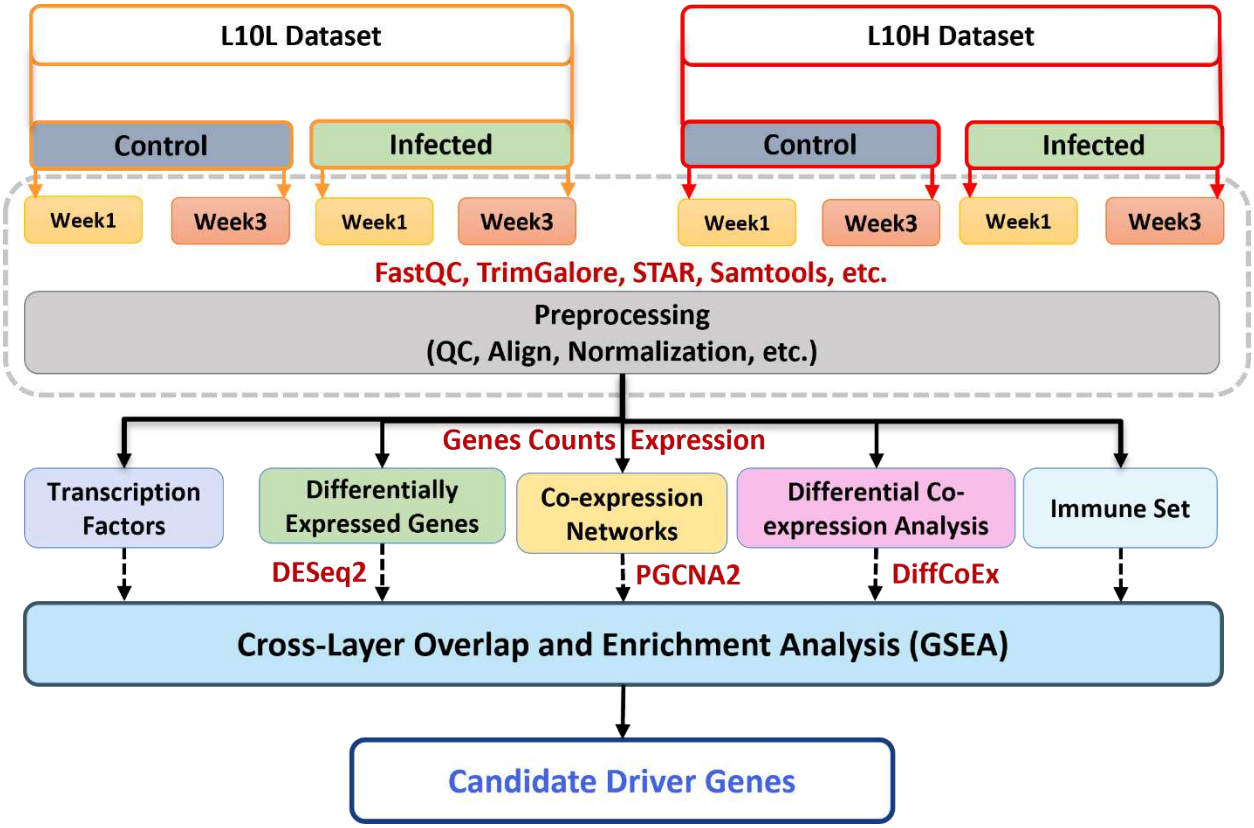


Figure 1. *Overall analytical workflow. Schematic of the integrative systems-level framework applied to the week-1 post-infection spleen transcriptomes: differential expression (DESeq2), parsimonious co-expression network construction (PGCNA2) and module detection, differential co-expression (link-based DCL/DCG test), transcription-factor annotation, and immune-phenotype association, whose integration (candidates require ≥3 of five criteria) prioritises candidate genes.*

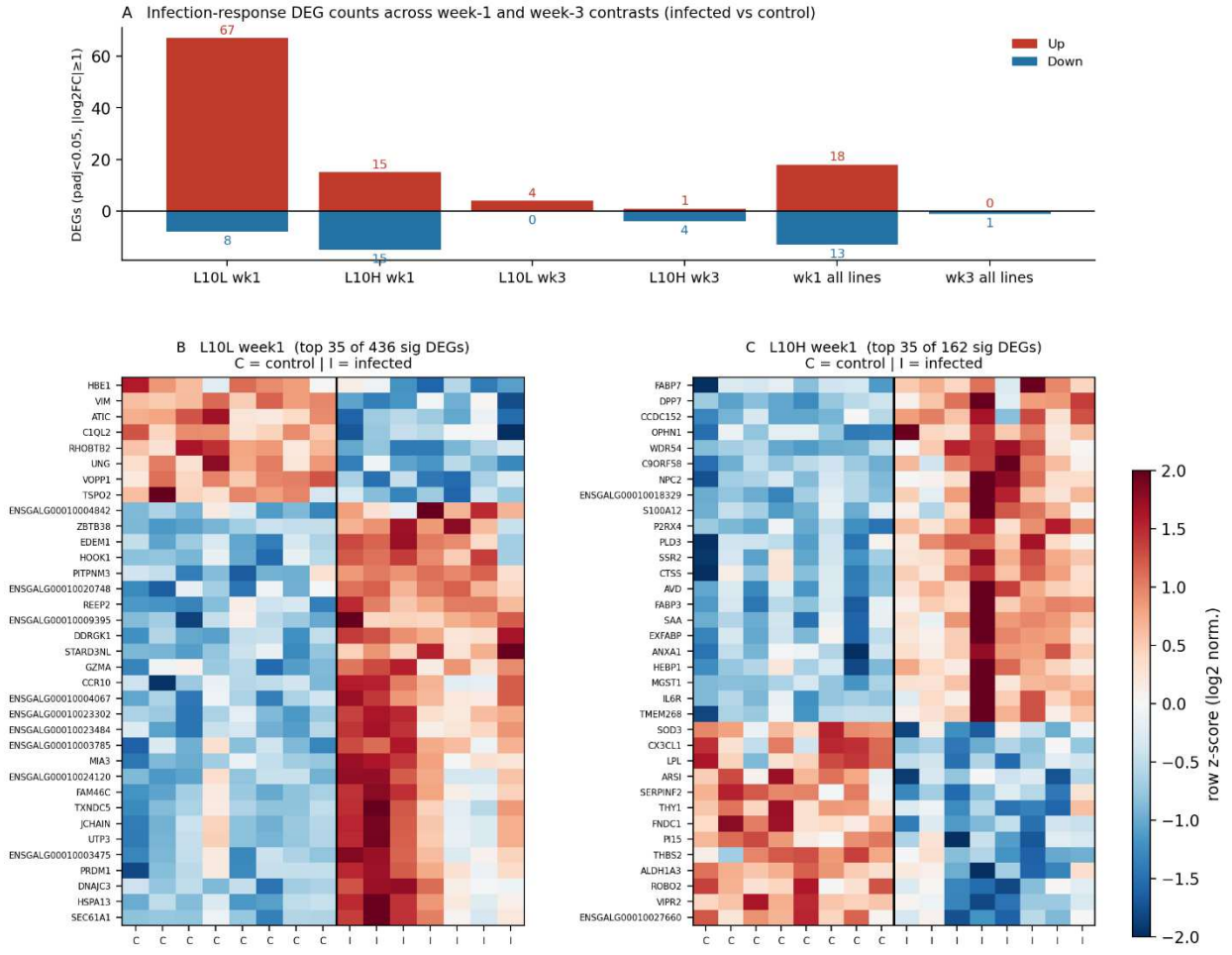


Figure 2. *Early (week-1) infection-response differential expression. (A) Numbers of up- and down-regulated DEGs (padj < 0.05, |log2FC| ≥ 1) across the week-1 and week-3 infection contrasts. (B,C) Heatmaps of the top significant infected-vs-control DEGs (padj < 0.05) in L10L and L10H; rows are genes (symbols), columns are that line's week-1 control (C) and infected (I) samples, colour is the per-gene z-score of log2-normalised expression.*

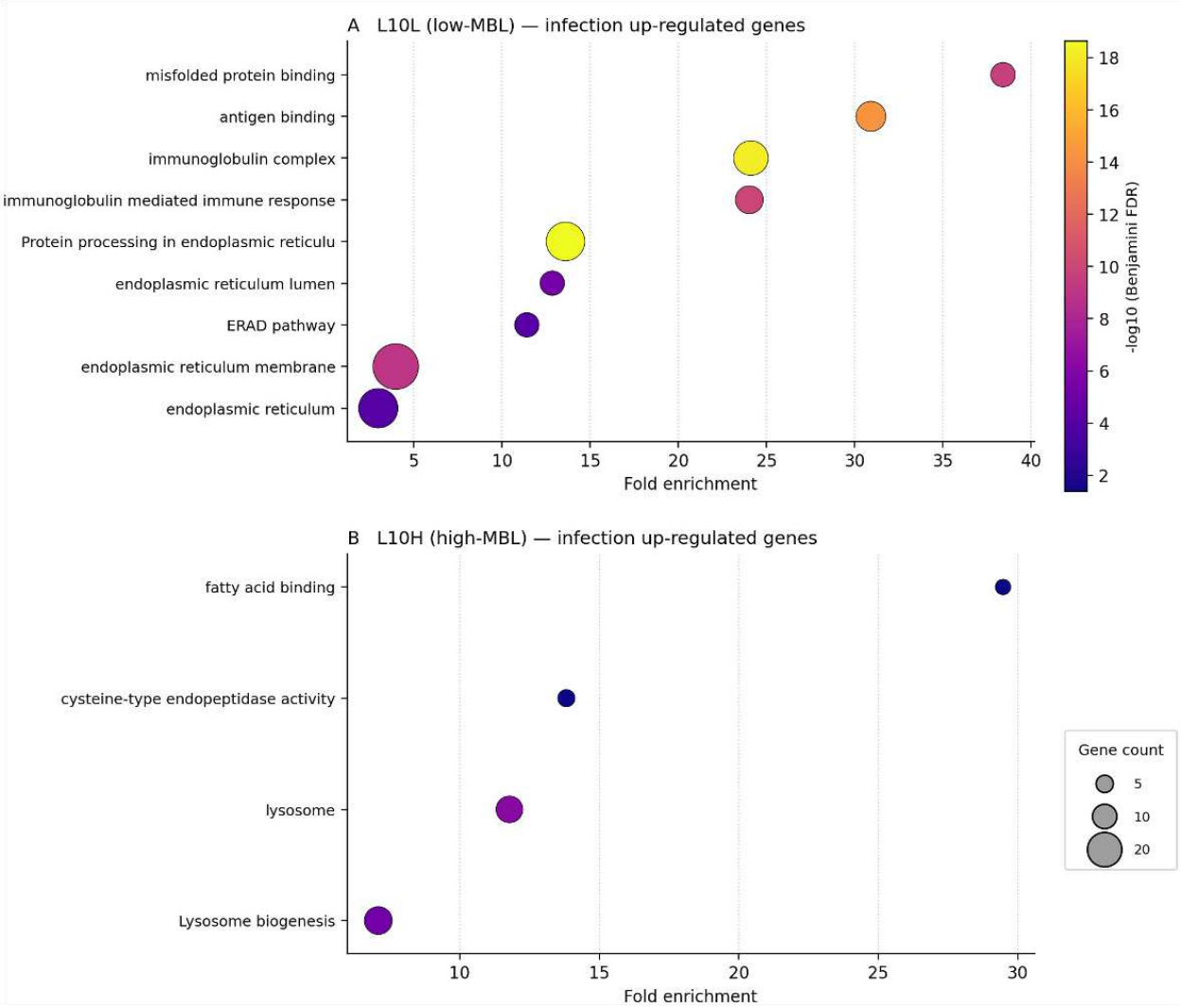
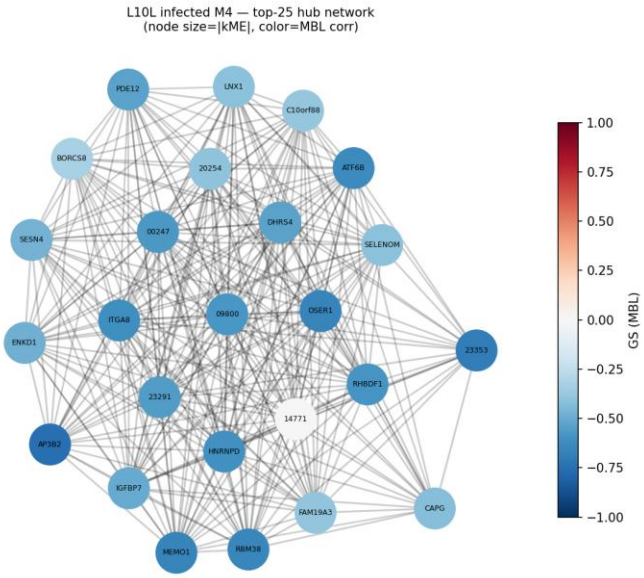
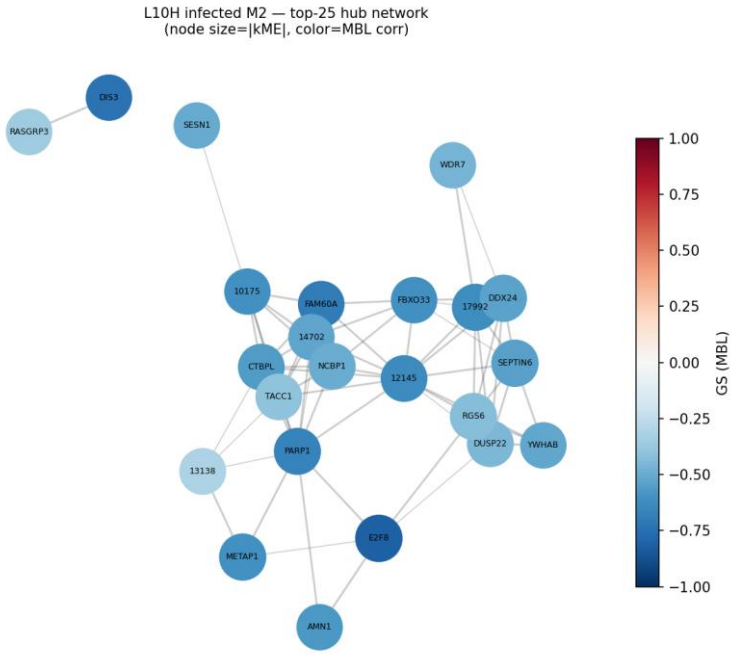


Figure 3. *Bubble plots of the top enriched pathway and Gene Ontology terms among up-regulated genes (infected vs control, week 1) in (A) the low-MBL line L10L and (B) the high-MBL line L10H. The x-axis shows fold enrichment, bubble size is proportional to the number of genes contributing to each term, and colour indicates statistical significance (–log10 Benjamini-adjusted P). The L10L response is dominated by immunoglobulin/antigen-binding and endoplasmic-reticulum protein-processing terms, consistent with an adaptive/antibody programme, whereas the L10H response is enriched for lysosomal and cysteine-type endopeptidase (cathepsin) terms, consistent with an innate, lysosomal antigen-processing programme.*



586

587 **Figure 4A.** *L10L infected module M4 hub network.*



588

589 **Figure 4B.** *L10H infected module M2 hub network.*

590 ***Figure 4.*** *Hub-gene networks of the MBL-anticorrelated infected modules. (A) L10L module M4*
591 *and (B) L10H module M2. Node size is proportional to module membership (kME); node colour*
592 *indicates each gene's Spearman correlation with baseline serum MBL. E2F8 is the dominant*
593 *L10H hub (kME = 0.97; MBL ρ = −0.82).*

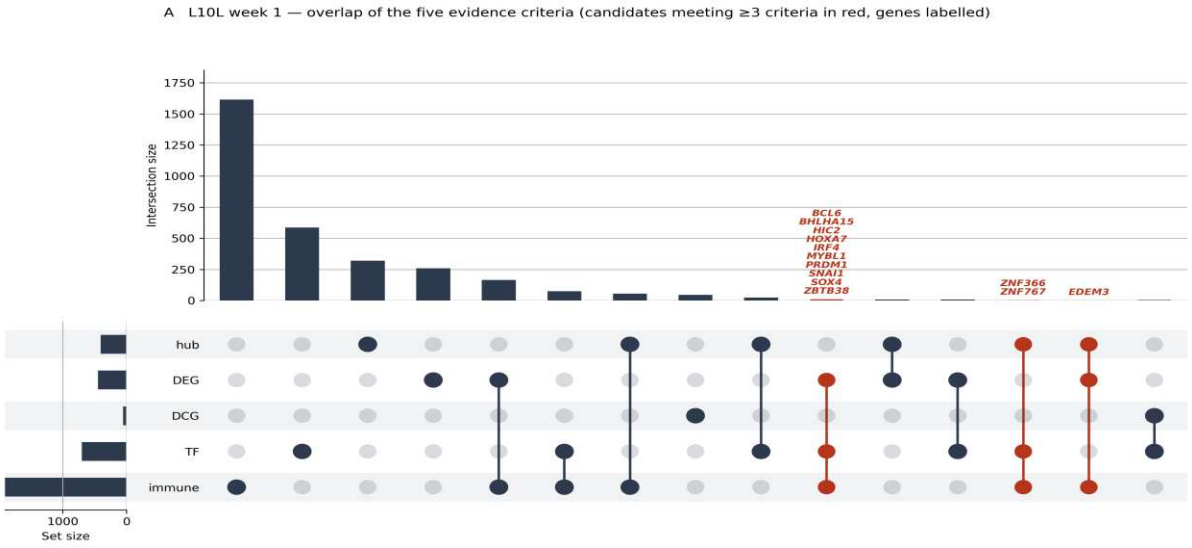


Figure 5A. L10L five-criterion overlap.

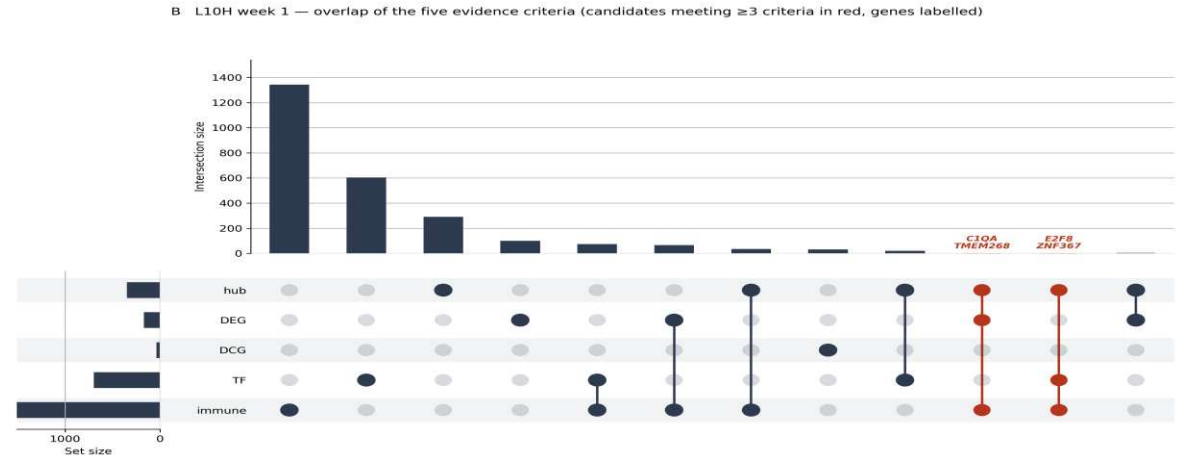
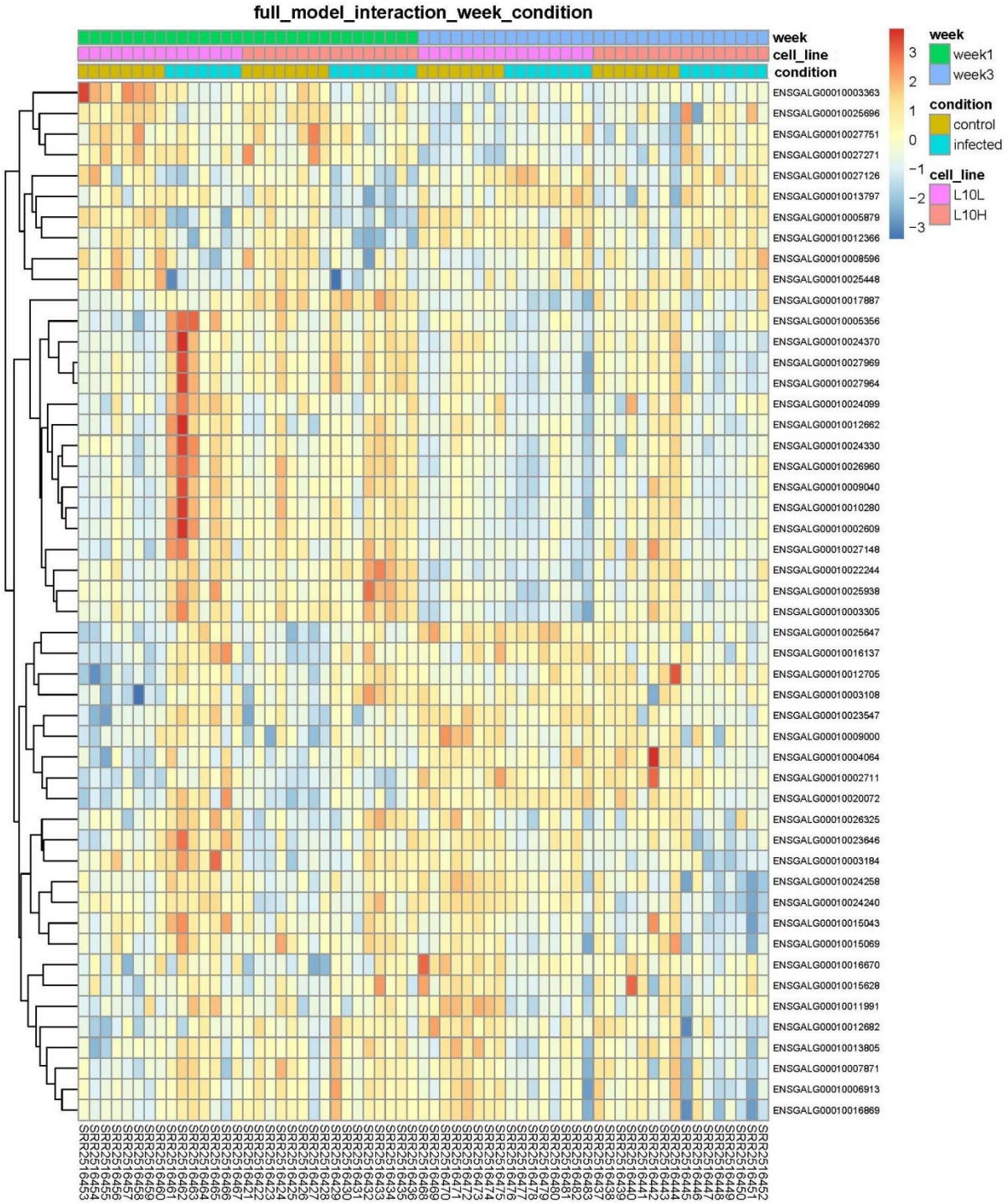


Figure 5B. L10H five-criterion overlap.

Figure 5. *Overlap among the five evidence criteria (UpSet). (A) L10L and (B) L10H. Rows are the five criteria (hub, DEG, DCG, TF, immune-trait-associated); top bars and matrix show each intersection and its size, with set sizes at the left. Intersections meeting at least three criteria are shown in red and their candidate genes are labelled; no candidate meets the DCG criterion.*

Supplementary Files:

Supplementary Fig. S1.



Supplementary Table.

Table S1. Evidence criteria met by each prioritised candidate gene (week 1). ✓, criterion met; –, not met. No candidate met the differential co-expression (DCG) criterion.

Line	Gene	Hub	DEG	DCG	TF	Immune-trait-associated
L10L	ZBTB38	–	✓	–	✓	✓
L10L	PRDM1	–	✓	–	✓	✓
L10L	EDEM3	✓	✓	–	–	✓
L10L	ZNF366	✓	–	–	✓	✓
L10L	BHLHA15	–	✓	–	✓	✓
L10L	SOX4	–	✓	–	✓	✓
L10L	SNAI1	–	✓	–	✓	✓
L10L	MYBL1	–	✓	–	✓	✓
L10L	HOXA7	–	✓	–	✓	✓
L10L	ZNF767	✓	–	–	✓	✓
L10L	BCL6	–	✓	–	✓	✓
L10L	HIC2	–	✓	–	✓	✓
L10L	IRF4	–	✓	–	✓	✓
L10H	C1QA	✓	✓	–	–	✓
L10H	E2F8	✓	–	–	✓	✓
L10H	TMEM268	✓	✓	–	–	✓
L10H	ZNF367	✓	–	–	✓	✓